Towards Heading Control of an Autonomous Sailing Platform through Weight Balancing

He, Jiaxi; Xiao, Lin; Jouffroy, Jerome

Publication date:
2012

Document version:
Submitted manuscript

Towards Heading Control of an Autonomous Sailing Platform through Weight Balancing

Jiaxi He * **Lin Xiao** ** **Jerome Jouffroy** **

Mads Clausen Institute, University of Southern Denmark (SDU),
Alsion 2, DK-6400, Sønderborg, Denmark

* *jiaxihe1989@gmail.com*
** {*xiao,jerome*}*@mci.sdu.dk*

Abstract: Autonomous sailing platforms or sailing robots are a class of autonomous surface vehicles using only the wind as their means of propulsion. In order to adapt to harsh conditions at sea, a robust design of an autonomous sailing platform is presented in this paper. The proposed sailing robot consists of a hull to which are attached a fixed and rigid sail, and an internal moving weight system used for steering. The control objective is to maintain a desired heading angle for the platform by automatically controlling the movable mass. Two different weight balancing mechanisms, i.e. a so-called linear weight mechanism and a pendulum mechanism, are introduced together with the mathematical model of the vehicle, exposed to ocean currents and wind variations. Furthermore, to allow maneuverability, dimensioning of the mass weight and the vehicle beam (or the pendulum length) are considered through simple nonlinear controllability properties using flatness theory. Finally, we present an exponentially stable heading controller based on backstepping and contraction theory, and which explicitly takes into account the presence of currents.

Keywords: Autonomous sailing vehicles; weight balancing; contraction theory; backstepping; heading control; flatness theory.

1. INTRODUCTION

Ocean observation and monitoring are some of the main purposes of autonomous sailing platforms, which can be seen as a complementary tool to other technologies available in ocean sampling (refer to Cruz and Alves (2008) and the references therein). Thanks to their clean technological and energy saving potentials, autonomous sailing robots were investigated more intensively in recent years (see *RoboSail* in Van Aartrijk et al. (1999), *IBOAT* in Briere (2008), and *FASt* in Cruz and Alves (2010)).

Until now, there are only a few studies on the automation of sailing tasks. Van Aartrijk et al. (1999) took the latest developments in the fields of Artificial Intelligence to the high seas, aiming to create a semiautonomous, intelligent computer system to steer a sailboat. In Briere (2008), sail tuning and rudder control are interpreted as a set of fuzzy rules that are then combined into a fuzzy controller. Cruz and Alves (2010) contributes with a simple model relating the most important variables (i.e. the yaw angle and the main torque input provided by the rudder) and concentrates on data that can be easily available with simple low-cost sensors. More recently, Xiao and Jouffroy (2011) proposed a nonlinear heading controller whose stability properties are investigated. However, most of these studies consider sailing vehicles with conventional appendages, i.e. one or two sails (with a typical bermuda rig) and a rudder.

Ideally, an unmanned sailing platform should be designed for operation at sea over a long period of time, and is expected to perform regularly in all circumstances, i.e. including harsh conditions. Arguably, sailing robots with conventional rigs could be vulnerable to extreme weather conditions. In this case, minimizing moving parts on the vehicle is of interest for robustness considerations. In this paper, we consider the scenario whereby the sail, a rigid wing, is assumed to be blocked or fixed in the middle position, while a weight balancing system inside the rigid body is the only means available for steering.

The remainder of this paper is organized as follows. Section 2 provides an overview of the background regarding autonomous sailing and motivations for the above-mentioned robust weight balancing steering mechanism/design. In section 3, we consider mathematical models of two different weight balancing mechanisms appended to the 4 DOF nonlinear dynamic model of a sailing vehicle derived in Xiao and Jouffroy (2011), together with the addition of ocean currents. In section 4, we sketch how –through simple nonlinear controllability considerations on the roll dynamics using flatness theory– the dimensions of the length of the beam and the weight of the mass could be deduced to increase maneuverability. Afterwards, heading control algorithms for both weight balancing mechanisms, based on backstepping and contraction theory, are presented. In order to illustrate the potential of our approach, the last part of section 4 is dedicated to a few simulation results.

Section 5 gives a few concluding remarks and possible research directions of interest.

2. MOTIVATIONS

Instead of deploying sensors from research ships for ocean observation, many alternatives have been developed, aiming at reducing the reliance on human intervention and labor cost of collecting data, among which are floats and drifters (see Roemmich et al. (2004) and Jouffroy et al. (2011)). They can provide real-time oceanographic data as they drift with ocean currents. However, the location of their measurements are hard to control and, to some extent, unpredictable.

As a consequence, autonomous underwater vehicles (AUVs) are broadly developed and autonomous underwater gliders have proven to be a powerful tool in ocean sampling because they are reusable, relatively inexpensive and can achieve missions of several months (see Bender et al. (2008) and Leonard and Graver (2001)). It seems that there is comparatively slightly less activity for autonomous surface vehicles, especially with wind-propelled sailing vehicles, even though the past few years saw a significant growth in this regard (among the studies on sailing robot design, see the interesting paper Neal (2006)).

Many existing autonomous surface vehicles used for ocean observation and monitoring are electrically or combustion engine propelled, which rely too much on batteries and thus have a relatively short life expectancy, potentially resulting in a significant cost due to maintenance and redeployment. Therefore, autonomous vehicles that are wind-driven are an attractive prospect. Indeed, their need for electrical energy only comes from onboard electronics and rudder control, resulting in the possibility of long term missions.

In Philpott et al. (1991), it is mentioned that the asymmetry of a small boat caused by the weight of crew can bring a righting moment. Apart from that, the weight asymmetry may also raise the yaw moment and can be used for steering. In addition, the control strategy of changing the internal mass position for the autonomous underwater gliders has been investigated in Leonard and Graver (2001). Similarly for an autonomous surface sailing robot, we can develop a weight balancing system, and then the orientation of the sailing platform is controlled only by the position of the weight inside the vehicle.

Furthermore, the sails on a regular sailing vehicle are flapping with the wind all along, which would result in the mechanical fatigue of the rigging, and even worse resulting in the rig breaking down. When an autonomous sailing robot sets out to operate for months at sea, it is very likely to be exposed to extreme weather. The problem in this case, and for monitoring platform applications, is that the appendages of the sailing platform, i.e. the sails and the rudder can after some time and harsh conditions be damaged by the marine environment, resulting again in a relatively short life expectancy. As a result, we turn to other alternative means of steering that is independent of the sail and rudder. Towards a robust design for an autonomous surface sailing platform, we propose in the present paper that the vehicle consists of a single rigid body with both the sail and rudder rigid and fixed, and an internal movable mass moving along the transverse plane of the vehicle, which increases the life of the autonomous sailing platform and requires very little maintenance.

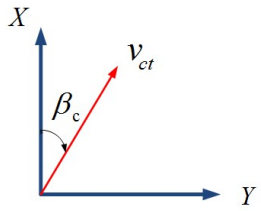

Fig. 1. Current velocity in 2-dimension

3. MODELING

In this section, we investigate the weight balancing mechanisms and establish the corresponding mathematical models by taking into account two different means of moving mass systems.

Using Fossen's compact notation for marine vehicles (Fossen (2011)) and based on the 4 DOF dynamic model of the sailing yachts derived in Xiao and Jouffroy (2011):

$$\begin{cases} \dot{\boldsymbol{\eta}} = \mathbf{J}(\boldsymbol{\eta})\boldsymbol{\nu} & (1) \\ \mathbf{M}\dot{\boldsymbol{\nu}} + \mathbf{C}(\boldsymbol{\nu})\boldsymbol{\nu} + \mathbf{D}(\boldsymbol{\nu},\boldsymbol{\eta}) + \mathbf{g}(\boldsymbol{\eta}) = \boldsymbol{\tau} + \boldsymbol{\tau}_w & (2) \end{cases}$$

where $\boldsymbol{\eta} = [x, y, \phi, \psi]^T$ denotes the position and orientation in the earth-fixed frame (i.e. the North-East-Down coordinate system), $\boldsymbol{\nu} = [u, v, p, r]^T$ describes the generalized velocity decomposed in the body-fixed frame in surge, sway, roll, and yaw, respectively. The expressions for the system inertia matrix $\mathbf{M}$, the coriolis-centripetal matrix $\mathbf{C}$, the damping vector $\mathbf{D}$, the vector of restoring forces $\mathbf{g}$, the sail and rudder forces $\boldsymbol{\tau}$, and the transformation matrix $\mathbf{J}$ are given in Xiao and Jouffroy (2011). More specifically, the heel-damping moment and the yaw-damping moment, which prevent the yacht from oscillating endlessly when it is rotating in the roll and yaw motions, together with the forces from the keel and the hull account for the damping vector $\mathbf{D}$ in (2). The sail angle and the rudder angle, which were considered as the control inputs for a conventional sailing yacht, are kept zero in the present paper as for the specific design of the sailing platform, and the forces and moments generated from the sail and rudder are grouped in $\boldsymbol{\tau}$. The vector $\boldsymbol{\tau}_w$ represents the control input from the autonomous moving weight.

In the following studies, we consider the motion of the sailing robot is influenced by the ocean currents. For irrotational ocean currents described by the magnitude v_{ct} and angle β_c in the horizontal earth-fixed frame (see Fig.1), the current velocity vector can be described as:

$$[u_c^E, v_c^E] = [v_{ct}\cos(\beta_c), v_{ct}\sin(\beta_c)] \quad (3)$$

u_c^E and v_c^E represent the current components in the North and East direction, respectively. Applying the rotation matrix, the current in the body-frame is:

$$\begin{bmatrix} u_c \\ v_c \end{bmatrix} = \mathbf{J}_c \begin{bmatrix} u_c^E \\ v_c^E \end{bmatrix} \quad (4)$$

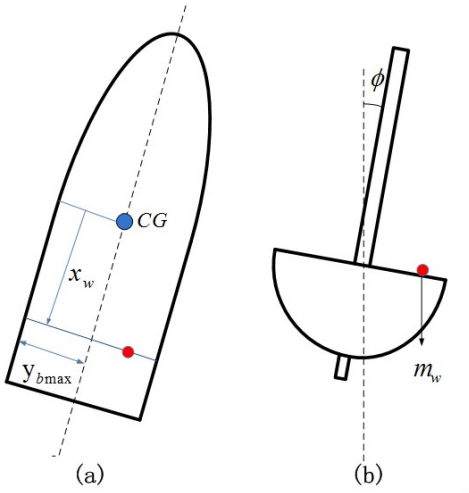

Fig. 2. Laterally movable weight model in the (a) plane view and (b) back view

where

$$\mathbf{J}_c = \begin{bmatrix} \cos\psi & \sin\psi \\ -\sin\psi\cos\phi & \cos\psi\cos\phi \end{bmatrix}$$

Consequently, for irrotational constant ocean currents, the vector of body-fixed current velocities is

$$\boldsymbol{\nu}_c = [u_c, v_c, 0, 0]^T$$

and $\dot{\boldsymbol{\nu}}_c = 0$. According to Fossen (2011), the equation of motion can be represented in terms of the relative velocity $\boldsymbol{\nu}_r = \boldsymbol{\nu} - \boldsymbol{\nu}_c$:

$$\begin{cases} \dot{\boldsymbol{\eta}} = \mathbf{J}(\boldsymbol{\eta})\boldsymbol{\nu} & (5) \\ \mathbf{M}\dot{\boldsymbol{\nu}} + \mathbf{C}(\boldsymbol{\nu}_r)\boldsymbol{\nu}_r + \mathbf{D}(\boldsymbol{\nu}_r, \boldsymbol{\eta}) + \mathbf{g}(\boldsymbol{\eta}) = \boldsymbol{\tau} + \boldsymbol{\tau}_w & (6) \end{cases}$$

To derive the expression of $\boldsymbol{\tau}_w$ in (6), two weight balancing models are discussed in the following subsection.

3.1 Linear Weight Model

As shown in Fig.2, the red point denotes an on-board moving weight, which is designed to move laterally from starboard to port. Fig.2(b) provides us a back view of the sailing platform, indicating that when the weight moves to the right side of the vehicle, it contributes a positive rolling moment, while on the other side resulting in a negative rolling moment. Thus, the movable weight contributes to an input vector $\boldsymbol{\tau}_w = [0, F_{yw}, M_{xw}, M_{zw}]^T$, and (refer to Xiao and Jouffroy (2012)):

$$F_{yw} = m_w \sin\phi \quad (7)$$

$$M_{xw} = y_w m_w y_{bmax} \cos\phi \quad (8)$$

$$M_{zw} = -y_w m_w |x_w| \sin|\phi| \quad (9)$$

where, y_{bmax} is half of the maximum yacht beam; x_w is the weight coordinate along the longitudinal axis, which is negative from Fig.2(a); y_w is the weight position relative to the vehicle center-line along the lateral axis in the body-frame, which ranges from -1 to 1. By introducing the saturation on the control input y_w, the singularity problem that might be caused by $\phi = 0$ would be avoided, since $y_w = \frac{M_{zw}}{-m_w|x_w|\sin|\phi|}$ from (9).

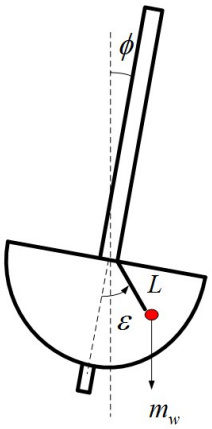

Fig. 3. Sketch of the pendulum work principle

3.2 Pendulum Model

The pendulum model is also a weight balancing system by re-devising the on-board weight into a pendulum. As seen in Fig.3, the length L of the pendulum is fixed, and we only need to control the tilt angle ε with respect to the vertical axis of the vehicle. When $\varepsilon = \phi$, the pendulum is vertical, and $\boldsymbol{\tau}_w = 0$.

In this case, the vector $\boldsymbol{\tau}_w = [0, F_{yw}, M_{xw}, M_{zw}]^T$ in (6) should be recalculated as below,

$$F_{yw} = m_w \cos(\varepsilon - \phi)\sin\varepsilon \quad (10)$$

$$M_{xw} = L m_w \sin(\varepsilon - \phi) \quad (11)$$

$$M_{zw} = -m_w \cos(\varepsilon - \phi)\sin\varepsilon |x_w| \quad (12)$$

Here, the singularity caused by $\phi = 0$ is avoided.

4. CONTROL THEORY FOR DIMENSIONING AND REGULATION

For both the linear weight model and the pendulum model, the control inputs (i.e. y_w and ε) are assumed to be saturated. In the linear weight model, y_w is bounded within [-1, 1], thus the maximum roll and yaw moments generated by the weight are described by the following inequalities

$$\begin{cases} -m_w y_{bmax} \le M_{xw} \le m_w y_{bmax} & (13) \\ -m_w x_w \le M_{zw} \le m_w x_w & (14) \end{cases}$$

Similarly, in the pendulum model, ε is constrained within $[-\frac{\pi}{2}, \frac{\pi}{2}]$, so we have:

$$\begin{cases} -L m_w \le M_{xw} \le L m_w & (15) \\ -m_w x_w \le M_{zw} \le m_w x_w & (16) \end{cases}$$

Thus, from (13)-(16), the maximum roll and yaw moments are related to m_w, x_w, y_{bmax} and L. Once x_w is determined, the dimensions of the mass and the beam length (or the mass and the pendulum length) can be adjusted according to the turning moments required, leading to higher maneuverability of the autonomous sailing platform.

4.1 Dimensioning

To begin with, we analyze the controllability of the roll dynamics using flatness theory (see Fliess et al. (1995)). The roll dynamics is derived from (5)-(6), and is given by

$$\dot{\phi} = p \tag{17}$$

$$\dot{p} = \frac{1}{I_{xx} + a_{44}}[\boldsymbol{\tau}_s(3) + \boldsymbol{\tau}_r(3) + M_{xw} - \boldsymbol{g}(3) - \boldsymbol{D}(3)] \tag{18}$$

where $I_{xx} + a_{44} > 0$. Substitute the expressions of $\boldsymbol{\tau}_s(3)$, $\boldsymbol{\tau}_r(3)$, $\boldsymbol{g}(3)$ and $\boldsymbol{D}(3)$ from Xiao and Jouffroy (2011), together with M_{xw} expressed in (8)(i.e. for the linear weight model), we have:

$$\dot{\phi} = p \tag{19}$$

$$\begin{aligned}\dot{p} = \frac{1}{I_{xx} + a_{44}}[&-F_{yr}(\alpha_{ar}, v_{ar})z_r - F_{ys}(\alpha_{as}, v_{as})z_s \\ &-F_{yk}(\alpha_{ak}, v_{ak})z_k - F_{yh}(\alpha_{ah}, v_{ah})\cos\phi z_h \\ &-a\phi^2 - b\phi - c\dot{\phi}|\dot{\phi}|] \\ &+ \frac{1}{I_{xx} + a_{44}} y_w m_w y_{bmax} \cos\phi\end{aligned} \tag{20}$$

F_{yr}, F_{ys}, F_{yk} and F_{yh} are respectively the force of the flow on the rudder, sail, keel and hull, which are functions of the apparent flow velocity v_a (i.e. the relative velocity of the wind or water to the vehicle) and apparent flow angle α_a, with the subscripts r, s, k, and h denoting the specific part on the sailing platform. Constant coefficients a, b, and c are determined through experiments. Choosing the flat output $z_1 = \phi$, then

$$p = \dot{z}_1 \tag{21}$$

and

$$\begin{aligned}y_w = \frac{I_{xx} + a_{44}}{m_w y_{bmax} \cos z_1}[&\ddot{z}_1 + \frac{1}{I_{xx} + a_{44}}(az_1^2 + bz_1 \\ &+F_{ys}(\alpha_{as}, v_{as})z_s + F_{yr}(\alpha_{ar}, v_{ar})z_r + F_{yk}(\alpha_{ak}, v_{ak})z_k \\ &+ F_{yh}(\alpha_{ah}, v_{ah})\cos\phi z_h + c\dot{z}_1|\dot{z}_1|)]\end{aligned} \tag{22}$$

Since the states p, ϕ and the control input y_w are functions of z_1 and its derivatives, the system described in (19)-(20) is flat, or controllable in the sense of flatness theory.

Consider now the case that the sailing robot is traveling approximately perpendicular to the wind (which is called reaching in sailing), which brings a maximum rolling moment on the robot, thus requiring a force to compensate for the wind-generated moment and try to hold the sailing platform upright. By using of the parameters and data from Xiao and Jouffroy (2012), we can compute for the minimum product of m_w and y_{bmax} to guarantee $y_w \in [-1, 1]$ from (22). Once the dimensions of the weight and beam length are determined in the worst case as mentioned, they can be used in any scenario to prevent the sailing platform capsizing.

Similarly in the pendulum model, substitute M_{xw} from (11) into (18), and pick again the flat output $z_1 = \phi$, then

$$p = \dot{z}_1 \tag{23}$$

$$\begin{aligned}\sin(\varepsilon - z_1) = \frac{I_{xx} + a_{44}}{L m_w}[&\ddot{z}_1 + \frac{1}{I_{xx} + a_{44}}(az_1^2 + bz_1 \\ &+F_{ys}(\alpha_{as}, v_{as})z_s + F_{yr}(\alpha_{ar}, v_{ar})z_r + F_{yk}(\alpha_{ak}, v_{ak})z_k \\ &+ F_{yh}(\alpha_{ah}, v_{ah})\cos\phi z_h + c\dot{z}_1|\dot{z}_1|)]\end{aligned} \tag{24}$$

where the input signal ε can be solved from $\sin(\varepsilon - z_1)$. Note that $\sin(\varepsilon - z_1)$ is within [-1, 1], we consider again the scenario as mentioned for the linear weight model, leading to the determination of the dimensions of m_w and L.

4.2 Heading Controller

In this subsection, we aim to derive the heading controller with contraction theory (Lohmiller and Slotine (1998)) and backstepping. From (5)-(6), we get the heading/yaw dynamics:

$$\dot{\psi} = r\cos\phi \tag{25}$$

$$\begin{aligned}\dot{r} = \frac{1}{I_{zz} + a_{66}}[&(a_{11} - a_{22})u_r v_r - dr|r|\cos^3\phi \\ &+ M_{zw} + M_{zs} + M_{zr}]\end{aligned} \tag{26}$$

with I_{zz} the principle moment of inertia in yaw, a_{11}, a_{22}, and a_{66} are all positive values. Constant d represents the yaw-damping coefficient, and the moments in yaw generated from the sail, rudder, and movable mass are grouped in M_{zs}, M_{zr}, and M_{zw}, respectively. Make a change of coordinate and define the variable $\widetilde{\psi} = \psi - \psi_d$ to represent the error in heading, hence (25) becomes:

$$\dot{\widetilde{\psi}} = r\cos\phi \tag{27}$$

with the desired heading angle constant, such that the equilibrium point of system (26)-(27) is the origin.

Here the state is $[x_1, x_2]^T = [\widetilde{\psi}, r]^T$ and the control input is M_{zw}, with the expression

$$\begin{aligned}f(x_1, x_2, u_r, v_r, p, \phi) = \frac{1}{I_{zz} + a_{66}}[&(a_{11} - a_{22})u_r v_r - \\ &- dr|r|\cos^3\phi + M_{zr} + M_{zs}]\end{aligned}$$

Rewrite the heading/yaw dynamics in $[x_1, x_2]$,

$$\begin{cases}\dot{x}_1 = x_2\cos\phi & (28)\\ \dot{x}_2 = f(x_1, x_2, u_r, v_r, p, \phi) + \dfrac{1}{I_{zz} + a_{66}} M_{zw} & (29)\end{cases}$$

and follow the approach of backstepping using contraction theory from Jouffroy and Lottin (2002), set the desired state as

$$x_{2d} = -x_1\sec\phi \tag{30}$$

which guarantees (28) contracting in x_1. Expressing the deviation as

$$z_2 = x_2 - x_{2d} = x_2 + x_1\sec\phi \tag{31}$$

we obtain

$$\dot{x}_1 = -x_1 + z_2\cos\phi \tag{32}$$

and

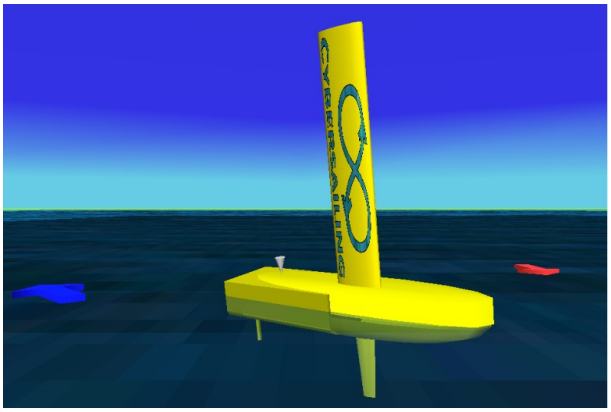

Fig. 4. Virtual representation of the sailing platform

$$\begin{aligned}\dot{z}_2 &= \dot{x}_2 + \dot{x}_1 \sec\phi + x_1 \frac{d}{dt}\sec\phi \\ &= f(x_1, x_2, u_r, v_r, p, \phi) + \frac{1}{I_{zz} + a_{66}} M_{zw} + x_2 \\ &\quad + x_1 p \tan\phi \sec\phi \end{aligned} \tag{33}$$

Thus, the desired control law M_{zw} is chosen as

$$\begin{aligned} M_{zw} = (I_{zz} + a_{66})[-f(x_1, x_2, u_r, v_r, p, \phi) - x_2 \\ - x_1 p \tan\phi \sec\phi - z_2 - x_1 \cos\phi] \end{aligned} \tag{34}$$

and the z_2-dynamics becomes:

$$\dot{z}_2 = -x_1 \cos\phi - z_2 \tag{35}$$

which shows that (35) contracting in z_2. By looking at the inter connections, one can check that the overall virtual displacement dynamics is:

$$\begin{bmatrix} \delta\dot{x}_1 \\ \delta\dot{z}_1 \end{bmatrix} = \begin{bmatrix} -1 & \cos\phi \\ -\cos\phi & -1 \end{bmatrix} \begin{bmatrix} \delta x_1 \\ \delta z_1 \end{bmatrix} \tag{36}$$

meaning that the heading/yaw dynamic system described in (25)-(26) is contracting. For different weight balancing models represented in (9) and (12), we are able to obtain the corresponding control laws y_w and ϵ from (34).

4.3 Simulation Reults

The results of the control laws derived above for each weight balancing model were simulated in Matlab Simulink.

The behavior of the linear weight model is visualized in a 3D graphic environment(see Fig.4), with parameters and lift and drag coefficients from Xiao and Jouffroy (2012). A standard Runge-Kutta method was employed to solve the equations of motion with a step size of 0.02 seconds. The wind is from the North and with a constant velocity 10 m/s, and the current is 1 m/s coming from the West. We started the simulation with initial values $[x, y, \phi, \psi, u, v, p, r]^T(0) = [0, 0, 0, 0, 0, 0, 0, 0]^T$, that is the sailing vehicle started turning while facing the wind.

As shown in Fig.5(a), the heading angle converges to the desired heading angle $\psi_d = 90$ deg. In Fig.5(c), the evolution of the control law y_w is presented, which maintains at 0.0035 in the steady state. The leeway angle converges to 2 deg from Fig.5(d).

To further verify the robustness of the controller by weight regulation on a sailing paltform, we add a stochastic

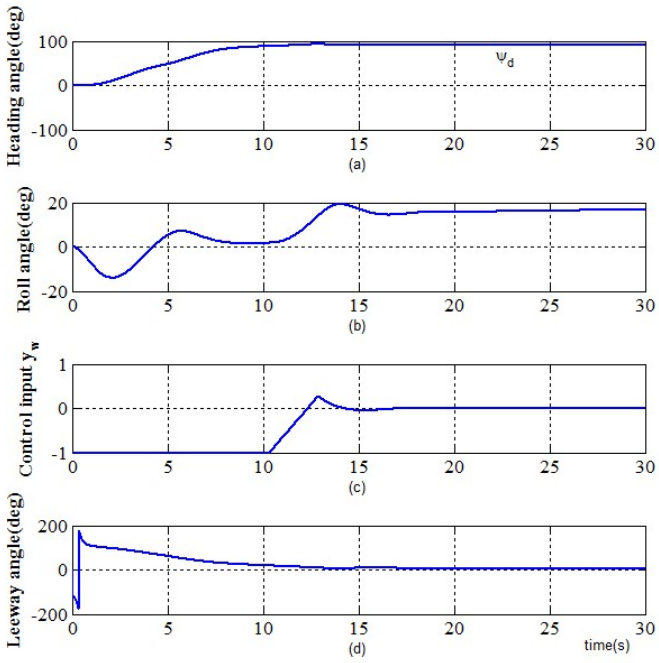

Fig. 5. Performance of the linear weight model

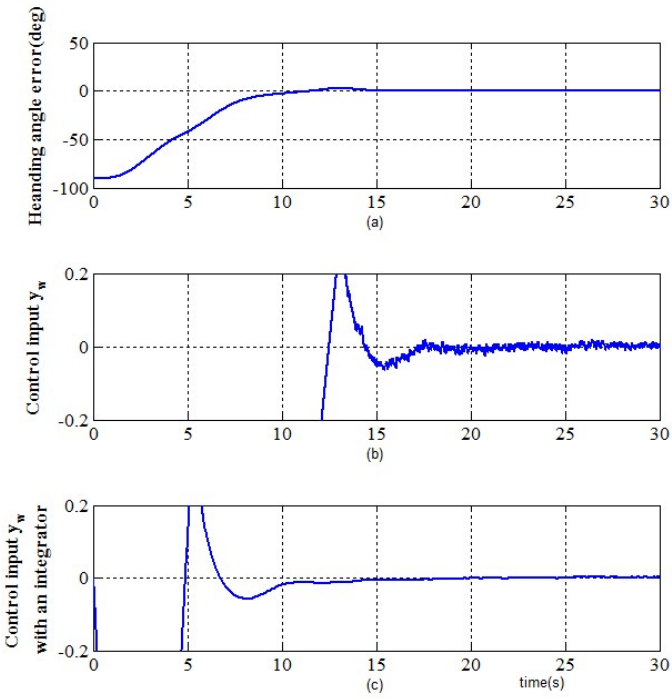

Fig. 6. Performance of the linear weight model in the presence of stochastic component

component to the current and wind, with the magnitude being 0.1 times as large as that of the wind and current. Fig.6(a) gives the heading angle error $\widetilde{\psi}$, which is bounded within 5e-4 deg, hence still exhibiting a good behavior. However, the changing rate of y_w is very fast as shown in Fig.6(b), so we put a slew rate limiter on y_w and add an integrator as in equation (39) to further smooth the input signal. Below is the new heading /yaw dynamics with an integrator:

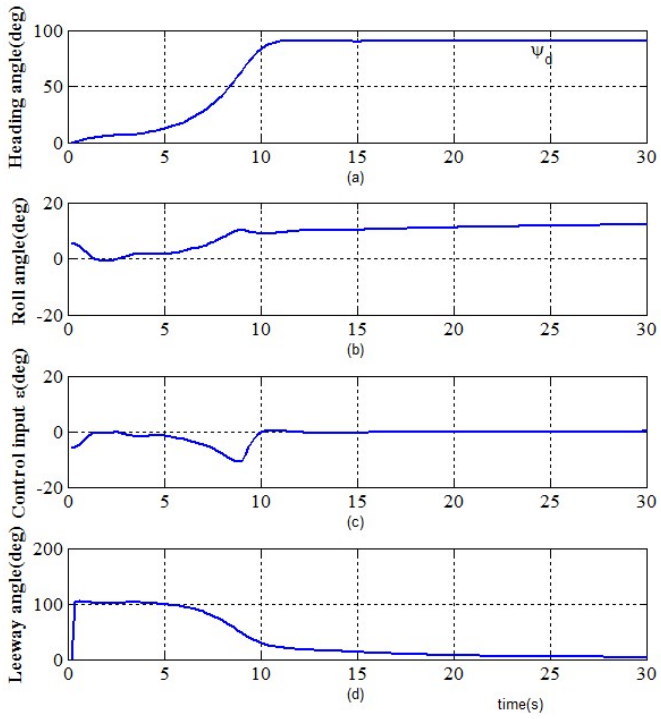

Fig. 7. Performance of the pendulum model

$$\begin{cases} \dot{x}_1 = x_2 \cos\phi & (37) \\ \dot{x}_2 = f(x_1, x_2, u_r, v_r, p, \phi) + \dfrac{m_w y_{bmax} \cos\phi}{I_{xx} + a_{44}} y_w & (38) \\ \dot{y}_w = u_w & (39) \end{cases}$$

Fig.6(c) presents performance of the linear weight model with an integrator and a slew rate limiter with rate 1. The frequency of y_w is much lower, while the error $\widetilde{\psi}$ is relatively bigger. Moreover, the bigger the slew rate, the lower the heading angle error is. Thus there is a trade-off between the choice of the slew rate and the error.

As for the simulation of the pendulum model, the initial value is chosen as $[x, y, \phi, \psi, u, v, p, r]^T(0) = [0, 0, 0, 0, 0, 0, 0, 0]^T$. It is indicated that ψ eventually converges to the desired heading angle from Fig.7(a). The final roll angle is approximately 14 deg from Fig.7(b). Fig.7(c) gives the evolution of ϵ, which approaches 0.03 deg in the end. Moreover, the leeway angle converges to 2 deg as shown in Fig.7(d).

5. CONCLUSION

The use of a robust autonomous sailing platform is proposed. Due to the work mechanisms of the sail and rudder, based on which the conventional heading controllers may fail to steer the vehicle in certain scenarios. As a compensation, we come up with two weight balancing models. In our model, the sail and rudder are rigid and fixed, while the state of the system is partially controlled using only the internal moving weight. Furthermore, the heading is successfully stabilized and controlled by applying the contraction theory and backstepping. From the simulations, the vehicle can be steered even when starting by facing the wind.

Our main focus for the near future is to introduce the wave disturbances in the motion model, and to implement the proposed controllers on an experimental platform.

REFERENCES

Bender, A., Steinberg, D.M., Friedman, A.L., and Williams, S.B. (2008). Analysis of an autonomous underwater glider. In *Proceedings of the Australasian Conference on Robotics and Automation,* pp. 1-10.

Briere, Y. (2008). IBOAT: An autonomous robot for long-term offshore operation. In *The 14th IEEE Mediterranean Electrotechnical Conference, MELECON,* Ajaccio(France), May, pp. 323-329.

Cruz, N. and Alves, J. (2008). Autonomous sailboat: an emerging technology for ocean sampling and surveillance. In *Proceeding of IEEE/MTS OCEANS,* Quebec City(Canada), Sept., pp. 1-6.

Cruz, N. and Alves, J. (2010). Auto-heading controller for an autonomous sailboat. In *Proceeding of IEEE/MTS OCEANS,* Sydney, May, pp. 1-6.

Fliess, M., Levine, J., Martin, P., and Rouchon, P. (1995). Flatness and defect of nonlinear system: Introductory theory and examples. In *International Jounal of Control*, VOL. 61, NO. 6, pp. 1327-1361.

Fossen, T.I (2011). *Handbook of Marine Craft Hydrodynamics and Motion Control.* John Wiley & Sons Ltd.

Jouffroy, J., Zhou, Q., and Zielinski, O. (2011). Towards selective tidal-stream transport for Lagrangian profilers. In *Proceeding of IEEE/MTS OCEANS*, Waikoloa, Sept.

Jouffroy, J. and Lottin, J. (2002). Integrator backstepping using contraction theory: a brief technological note. In *IFAC World Congress, Barcelona.*

Leonard, N. and Graver, J. (2001) Model-Based Feedback Control of Autonomous Underwater Gliders. In *IEEE Journal of oceanic engineering,* VOL. 26, NO. 4, pp. 633-645, Oct.

Lohimiller, W. and Slotine, J.E. (1998). On contraction analysis for non-linear systems In *Automatica,* VOL. 34, NO. 6, pp. 683-696.

Neal, M. (2006). A hardware proof of concept of a sailing robot for ocean observation. In *IEEE Journal of Oceanic Engineering,* VOL. 31, NO. 2, pp. 462-469.

Philpott, A., Sullivan, R. and Jackson, P. (1991). Yacht velocity prediction using mathematical programming In *European Journal of Operational Research, North-Holland.*

Roemmich, D., Riser, S., Davis, R. and Desaubies,Y. (2004). Autonomous profiling floats: workhorse for broad-scale ocean observations. In *Marine Technology Society Journal,* VOL. 38, NO. 1, pp. 31-39.

Van Aartrijk, M.L., Tagliola, C.P. and Adriaans, P.W. (1999). AI on the ocean: the robosail project. In *Proceedings of the 15th European Conference on Artificial Intelligence.*

Xiao, L. and Jouffroy, J. (2011). Modeling and nonlinear heading control for sailing yachts. In *Proceeding of IEEE/MTS OCEANS*, Waikoloa, Sept.

Xiao, L. and Jouffroy, J. (2012). Modeling and nonlinear heading control of sailing yachts. Submitted.